Available online at www.sciencedirect.com
ScienceDirect
Journal of Marine Systems 69 (2008) 283–294
JOURNAL OF MARINE SYSTEMS
www.elsevier.com/locate/jmarsys

Quantifying copepod kinematics in a laboratory turbulence apparatus

J. Yen [a,*], K.D. Rasberry [b], D.R. Webster [b]

[a] School of Biology, Georgia Institute of Technology, 310 Ferst Drive, Atlanta, GA 30332-0230, United States
[b] School of Civil and Environmental Engineering, Georgia Institute of Technology, Atlanta, GA 30332-0355, United States

Received 1 September 2005; received in revised form 20 December 2005; accepted 28 February 2006
Available online 1 March 2007

Abstract

We describe application of a new apparatus that permits simultaneous detailed observations of plankton behavior and turbulent velocities. We are able to acquire 3D trajectories amenable to statistical analyses for comparisons of copepod responses to well-quantified turbulence intensities that match those found in the coastal ocean environment. The turbulence characteristics consist of nearly isotropic and homogeneous velocity fluctuation statistics in the observation region. In the apparatus, three species of copepods, *Acartia hudsonica*, *Temora longicornis*, and *Calanus finmarchicus* were exposed separately to stagnant water plus four sequentially increasing levels of turbulence intensity. Copepod kinematics were quantified via several measures, including transport speed, motility number, net-to-gross displacement ratio, number of escape events, and number of animals phototactically aggregating per minute. The results suggest that these copepods could control their position and movements at low turbulence intensity. At higher turbulence intensity, the copepods movement was dominated by the water motion, although species-specific modifications due to size and swimming mode of the copepod influenced the results. Several trends support a dome-shaped variation of copepod kinematics with increasing turbulence. These species-specific trends and threshold quantities provide a data set for future comparative analyses of copepod responses to turbulence of varying duration as well as intensity.

Keywords: Copepod; Turbulence; Kinematics

1. Introduction

Some of the most provocative questions in biological oceanography are focused on the interaction of organisms and turbulence (e.g. Rothschild and Osborn, 1988; Saiz and Kiørboe, 1995; Dower et al., 1997; Incze et al., 2001; Franks, 2001). Small organisms in the ocean, such as copepods, are subject to fluid forces imposed by the turbulent velocity field. Copepods are similar in size (1–10 mm) to the range of smaller turbulent eddies (Jiménez, 1997) and move at speeds (1–10 mm s^{-1}) similar to small-scale velocity fluctuations (Yamazaki and Squires, 1996). Copepods appear well-suited for detecting and responding to small-scale turbulent motions. Copepods can detect small-scale velocity gradients via mechanoreceptors on their antennules that are separated at distances spanning μm to cm and are oriented along different planes, orthogonally or otherwise (Landry and Fagerness, 1988; Boxshall et al., 1997). The setae accurately encode the intensity and direction of fluid disturbances (Fields et al., 2002). Copepods have been observed to respond to nm displacements, μm s^{-1} flows, and 0.05 s^{-1} strain rates (Yen et al., 1992; Fields and Yen,

* Corresponding author. Tel.: +1 404 385 1596; fax: +1 404 894 0519.
E-mail address: jeannette.yen@biology.gatech.edu (J. Yen).

0924-7963/$ - see front matter © 2007 Elsevier B.V. All rights reserved.
doi:10.1016/j.jmarsys.2006.02.014

1997; Kiørboe et al., 1999; Visser, 2001; Titelman, 2001; Woodson et al., 2005). Copepods respond to threshold strain rates with directional escape responses to predator signals (Yen and Fields, 1992; Fields and Yen, 1997) and with area-restricted search behavior to thin layer structure (Woodson et al., 2005).

Impacts of turbulence on feeding rate, growth rate, survivorship, and predation pressure likely vary species-by-species (reviewed in Dower et al., 1997; Marrasé et al., 1997; MacKenzie, 2000; Peters and Marrasé, 2000), leading to the conclusion that the interaction of zooplankton with turbulence may be far more complicated than currently known or predicted (e.g., Jonsson and Tiselius, 1990; Saiz and Alcaraz, 1992; Yamazaki, 1996; Visser et al., 2001; Saiz et al., 2003; Galbraith et al., 2004; Lewis, 2005). One observed impact of turbulence is species-specific differences in the vertical distributions of planktonic copepods in relation to the physical structure of the water column (Heath et al., 1988; Haury et al., 1990; Mackas et al., 1993; Lagadeuc et al., 1997; Incze et al., 2001; Visser et al., 2001, Manning and Bucklin, 2005). Copepod distributions throughout the ocean are determined by many factors, including chemical, biological, and physical effects. Thus, it is difficult for field observations alone to determine the underlying causes of the species-specific differences, and in particular the role of individual behavioral responses to physical (e.g., turbulence, light, temperature, salinity); chemical (dissolved oxygen, nutrients), and biological cues (presence or absence of prey, predator, and competitor species).

While turbulence has been suggested as a factor that influences vertical partitions of some species of copepod, the role of animal behavior has been difficult to quantify. In a study on Georges Bank, Incze et al. (2001) observed that several species of copepods and their nauplii reacted strongly to the onset of wind, and thus turbulence, by moving below the mixed layer in just a few tens of minutes. Other studies have found similar results in other ocean regions (e.g. Heath et al., 1988; Haury et al., 1990; Mackas et al., 1993; Lagadeuc et al., 1997; Visser et al., 2001, Visser and Stips, 2002). These studies strongly suggest that in many oceanic regimes, turbulence affects the vertical position of copepods primarily by changing their behavior, and only secondarily by physically altering their position. A general expectation is that planktonic organisms are adapted to the conditions that they commonly experience (Incze et al., 2001). Copepods may be adapted to a specific level of ambient turbulence to improve encounter rate without loss of signal structure or range of perception. Copepods may seek calmer waters by sinking to deeper levels in the ocean as the surface becomes more turbulent, or alternatively may maintain their position in rough waters. Hence, the field data show an intriguing relationship of copepod distribution to turbulence level that appears driven both by the fluid motion and the behavioral response to the fluid motion. Recent research (Franks, 2001; Incze et al., 2001) points out that interpretation and prediction of zooplankton distributions in the ocean will follow only from a better understanding of animal responses to changing turbulence.

In the current study, we use a laboratory apparatus to simulate natural levels of turbulence to study the influence on the kinematics of three species of copepod, *Acartia hudsonica*, *Temora longicornis*, and *Calanus finmarchicus*. The flow characteristics in the observation region are stagnant water and four intensity levels of nearly isotropic and homogeneous turbulence. Here, we describe the potential that our turbulence apparatus has, in terms of acquiring 3D trajectories amenable to statistical analyses for comparisons of copepod responses to well-quantified turbulence intensities that match *in situ* conditions. We seek insight into the effect of turbulence on swimming behavior that influences vertical population distributions, predator–prey interactions, and other processes.

2. Methods

2.1. Physical environment

Experiments were performed in an apparatus (T-Box) that generates small-scale isotropic turbulence (fully described in Webster et al., 2004). The apparatus (0.4 m × 0.4 m × 0.4 m) was filled with artificial seawater created with filtered fresh water and Instant Ocean (30 ppt). Eight synthetic jet actuators, one located at each corner of the apparatus, generate the turbulent flow. Webster et al. (2004) quantified the velocity fields for a range of turbulent flow conditions described by the dissipation rate (10^{-3}–1 cm^2 s^{-3}) and Kolmogorov microscale (0.04–0.2 cm). These ranges agree well with that associated with the coastal zone and wind-driven turbulence (Granata and Dickey, 1991; Kiørboe and Saiz, 1995; Jiménez, 1997). The apparatus produces an appropriate range of length scales, velocity scales, and fluctuating strain rate levels for zooplankton mechanosensory studies (Webster et al., 2004).

The flow field at the center of the box was nearly statistically isotropic and homogeneous (Webster et al., 2004). For T0, the actuators were stationary and no active turbulent forcing was present, hence the fluid was essentially stagnant. For T1, T2, T3, and T4, the turbulent flow was created by using pre-determined amplification levels for each of the eight actuators.

Table 1
Turbulence characteristics from Webster et al. (2004)

Turbulence Level	1	2	3	4
ε (cm^2 s^{-3})	0.002	0.009	0.096	0.25
η (cm)	0.15	0.10	0.057	0.045
u_{rms} (mm s^{-1})	1.1	2.8	7.5	9.3
σ_{rms} (s^{-1})	0.11	0.24	0.79	1.2

Data shown are the average of the r.m.s. of velocity for each coordinate direction, u_{rms}, and the average of the r.m.s. of the linear components of the strain rate, σ_{rms}.

Table 1 summarizes the flow characteristics for each of the turbulence levels. The velocity r.m.s. value reported is the average of the three components reported in Webster et al. (2004). The strain rate r.m.s. value is the average of the linear strain rate components reported in Webster et al. (2004).

As shown in Fig. 1, the *X* and *Y* coordinates corresponded to the horizontal coordinates of the box, and *Z* was the vertical coordinate. All experiments were conducted in a dark laboratory room. To determine the effect of turbulence on a copepod behavior, we stimulated the phototactic response in the copepods. A light beam was projected vertically through the center of the box in order to evoke the phototactic response. The light source was the green line (514 nm) of a 100 mW laser (Uniphase).

2.2. Copepods tested

Three species of copepod were tested during the course of these experiments: *A. hudsonica*, *T. longicornis*, and *C. finmarchicus*, which are commonly collected in the western Gulf of Maine. Table 2 provides general characteristics for the copepod species. Manning and Bucklin (2005) observed that both *A. hudsonica* and *A. longiremis* occupied surface waters in May. In June and July, *A. hudsonica* was evenly distributed, while *A. longiremis* was most abundant in deep waters, which suggests a species-specific response. We also examined copepods with uniform vertical distribution (*T. longicornis*) vs. copepods whose abundance can peak during seasons of high turbulence (*C. finmarchicus*) and may be less sensitive to the mixing regime.

2.3. Behavior observation method

As our initial test of the system, we report copepod kinematics rather than their long-term feeding response. In this study, no food particles were added and hence we expected no variation in pursuit behavior. The objective of these preliminary tests was to isolate the pure mechano-reception response to turbulent environments without the confounding presence of food particles. Copepods in each region will have their own responses to turbulence, modified by other factors such as food levels, presence of predators, and season. By assessing the response to turbulence while these other factors were fixed, we isolated effects and evaluated the contribution due to turbulence alone.

We observed freely swimming copepods passing through the center region of the apparatus. A shadowgraph system was used to record copepod position. A translucent sheet of paper (100% rag vellum) was attached to the outside of each wall of the T-box facing the cameras. These sheets acted as the screen for the copepods′ shadow images. Illumination was provided by lasers operating in the red wavelengths, for which the tested copepods did not behaviorally respond. Opposite from the cameras a Melles–Griot red diode OEM laser was reflected off circular concave mirrors (Melles–Griot, 2000 mm focal length, 153 mm diameter, f/10) creating a wide column of laser light through the box center (Fig. 1). During the *C. finmarchicus* and *T. longicornis* experiments a 0.5 cm × 0.5 cm grid was printed on the vellum paper. Because *A. hudsonica* are smaller organisms, the grid interfered with trajectory and transport speed analysis. Therefore, plain vellum paper was used without a grid.

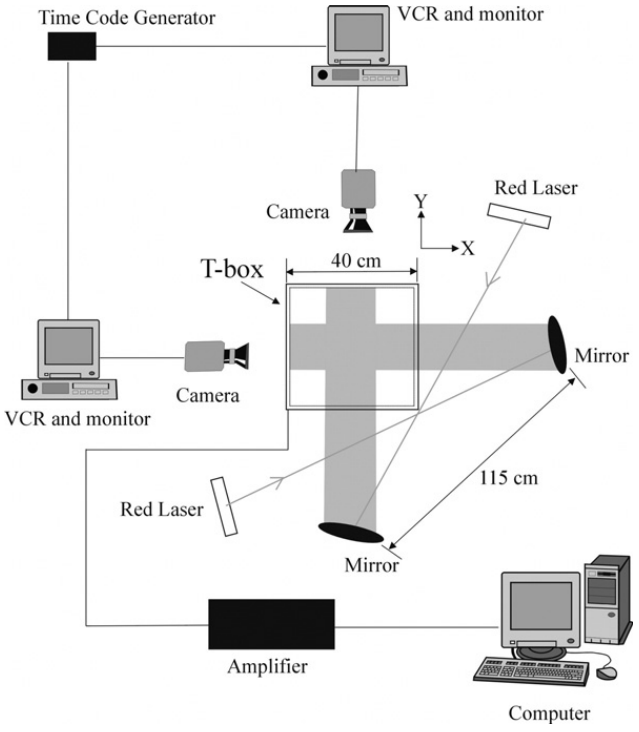

Fig. 1. Schematic of the experimental set-up during animal behavior measurements (top view).

Table 2
General characteristics of copepods tested

Species	Bodylength (mm)	Swim speed (mm s^{-1})	Sinking rate (mm s^{-1})	Habitats	Geography	Swim style
A. hudsonica	1	1–6[a]	0.4–2[d]	Coastal estuaries	N. Atlantic	Hop and sink
T. longicornis	1–3	2.7–6.1[b]	2.5[e]–2.9[f]	Continental shelf	Atlantic, Pacific	Cruise and sink
C. finmarchicus	4–5	2–5[b]	5[f]	Continental shelf	N. Atlantic	Cruise
		10[c]	♀1.9–2.2[g]			
			♂ 2.3–3.1[g]			

Data from Mauchline (1998), [a]Buskey et al. (1983), [b]Buskey and Swift (1985), [c]Hirche (1987), [d]Weissman et al. (1993), [e]Jonsson and Tiselius (1990), [f]Apstein (1910), [g]Gross and Raymont (1942). ♀,♂ = genders sink at different rates.

Two cameras viewed the T-box apparatus from perpendicular perspectives (Fig. 1). Hence, the cameras captured the *XZ* and *YZ* perspectives simultaneously. For the *C. finmarchicus* and *T. longicornis* experiments, the cameras were a Pulnix TM 745 (748 × 494 pixels) and a Hitachi KP-M1 (2/3 in. image chip size with 410,000 pixels), both with a 60 mm Nikon micro-Nikkor lens. The images were recorded via JVC VHS VCRs at 30 frames per second (fps). A Horita SMPTE Time Code Generator (TRG-50) simultaneously marked the time on the tapes. The cameras for the *A. hudsonica* experiments were Sony Mini DV Digital Handycams. The resolution was 640 × 480 pixels, and the recording speed was 60 fps. The camcorders for the *A. hudsonica* experiment have a viewing window and timer; hence the VCR, monitor, and time code generator were not needed.

The sequence of turbulence treatments was dictated by practical constraints during the experiments. In order to maintain a near constant temperature for the fluid in the apparatus, experiments were limited to a 3-hour period in which the temperature changed from 11 °C to 13 °C, thus bracketing the environmental temperature of 12 °C. Within this time period, we were able to run 5 turbulence levels with no replicates. Due to these limitations, we chose to expose copepods to increasing turbulence intensities, starting from still water through four intensities to a maximum at $\varepsilon = 0.25\ cm^2\ s^{-3}$. While fatigue, habituation, and overexposure of mechanosensors are factors that may confound our results, we can consider that copepods exposed to the highest turbulence level will be witnessing previous intensities. As most storms persist for more than 3 h, fatigue can be a prevailing condition for these copepods.

Prior to recording, each turbulence level condition was given sufficient time (approximately 10 min) for the flow to achieve fully isotropic and homogeneous conditions at the box center. Copepod positions were recorded for each T-level for roughly 20 min. During the first 5 min for each level there was no green light entering the T-box. At the 5 min mark, the green laser was turned on and the beam passed vertically through the center of the box for the remaining 15 min.

We have allowed the animals to adjust to each turbulence level for wait times of 5–10 min to allow for habituation. Hwang et al. (1994) stated that the copepod *Centropages hamatus* escaped more frequently during the first 6 min of initiated turbulence, and more than 50% of the total escape reactions occurred during this initial period.

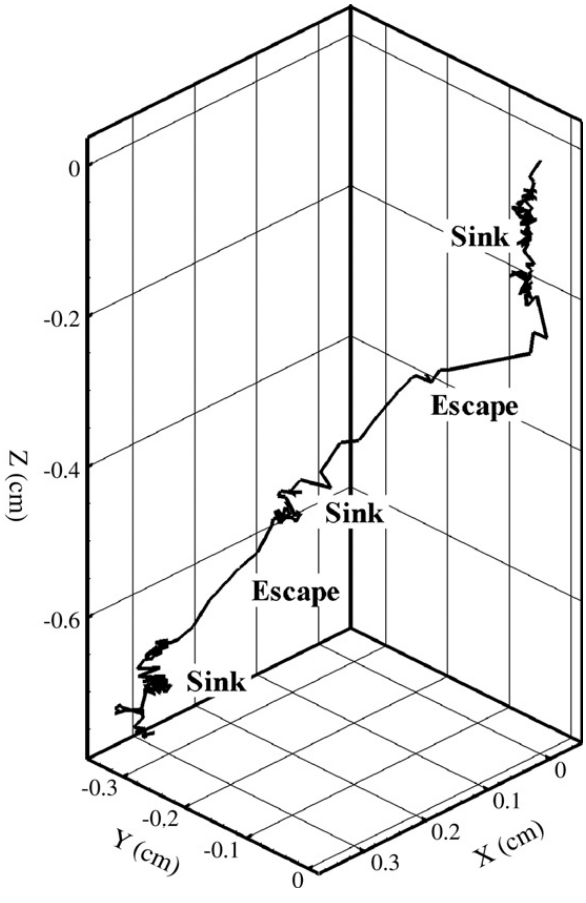

Fig. 2. Sample *A. hudsonica* trajectory for T0 including escape and sink patterns.

2.4. Copepod trajectory analysis

Three-dimensional trajectories were systematically extracted from the video recordings by digitizing the video tapes using ExpertVision software (MotionAnalysis Corp.) at 60 Hz. The recordings for the *XZ* and *YZ* perspectives were digitized separately. The *XZ* and *YZ* coordinates of a trajectory were then matched to fully define a three-dimensional trajectory. A sample trajectory is shown in Fig. 2. Path kinematics were subsequently calculated based on the three-dimensional trajectory relative to a fixed frame of reference. Quantified behavioral metrics include: observed transport speed, standard deviation of transport speed, motility number, net-to-gross displacement ratio, and number of escapes per time. For our estimates of the net-to-gross displacement ratio as a measure of path complexity (Dicke and Burrough, 1988), we analyzed 1-second trajectories for each species at each turbulence level.

Typically, 7 to 22 trajectories were collected for each species for each turbulence level. Each trajectory consisted of between 60 and 600 data points. To determine the number of trajectories needed in the calculation of speeds and other kinematic metrics, analyses of the standard error were performed. In all cases, enough trajectories were analyzed such that the standard error asymptoted to a constant low value (Rasberry, 2005).

2.5. Statistical analysis

We performed analyses of the skewness and kurtosis to test for homoscedasticity of the data. Data were transformed if found non-normal. We used two-way analysis of variance with species and strain rate as the main effects to assess the significance of these variables, and their interactions, on behavioral responses of copepods. Turbulence intensity is quantified here as strain rate, as this is a fluid mechanical signal perceivable by copepods (Yen and Fields, 1992). Because the strain rate is a fluctuating quantity in turbulence (with an average of zero for isotropic conditions), the r.m.s. of the strain rate provides a measure of the fluid mechanical signal. If the two-way analysis of variance showed a

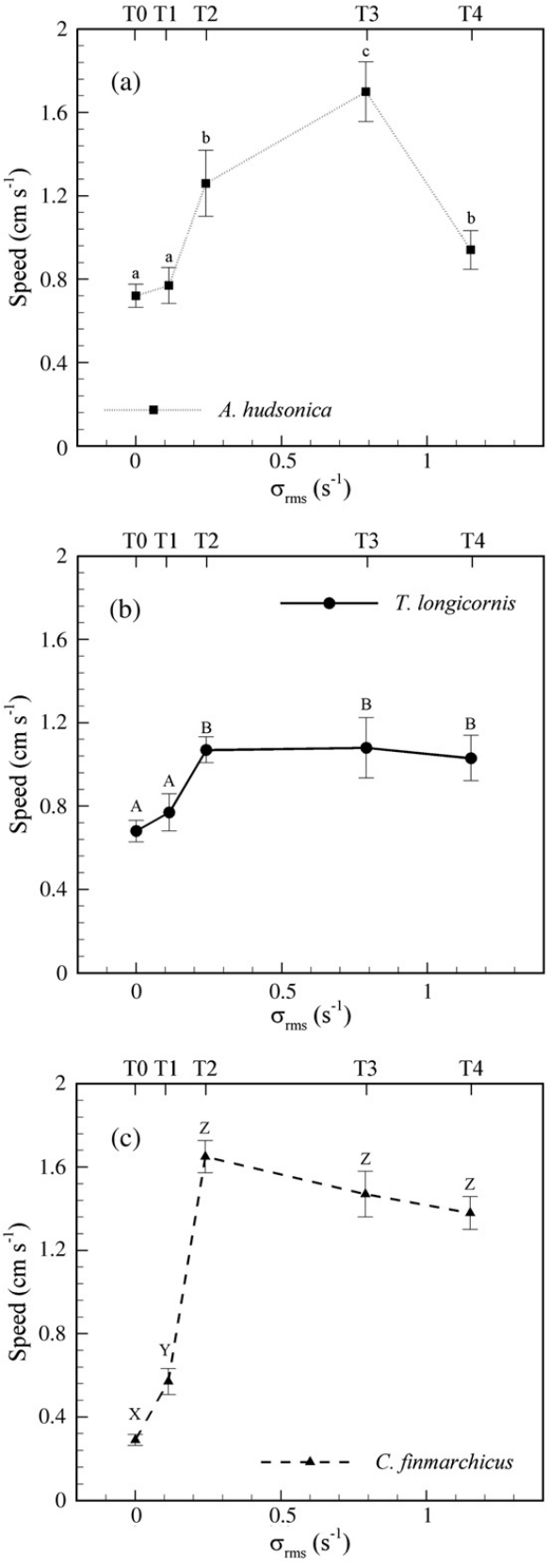

Fig. 3. Observed transport speeds for (a) *A. hudsonica*, (b) *T. longicornis*, and (c) *C. finmarchicus* as a function of r.m.s. of strain rate. Letters indicate treatments that are not significantly different using a Tukey–Kramer test, $p<0.05$. For *A. hudsonica*, treatment *a* is not significantly different from treatment *a*, treatment *b* is significantly different from treatment *a*, treatment *c* is significantly different from treatment *a* and treatment *b*. For *T. longicornis*, *A* is not significantly different from *A*, *B* is significantly different from *A*, *C* is significantly different from *A* and *B*. For *C. finmarchicus*, *X* is not significantly different from *X*, *Y* is significantly different from *X*, *Z* is significantly different from *X* and *Y*. This lettering scheme applies to all the Tukey Kramer LSD tests.

significant species * strain rate interaction, we performed a single factor analysis of variance to assess, for each species, the effect of strain rate on copepod behavior. This analysis allowed us to examine the role of turbulence when it may exert different effects on individual species. Tukey–Kramer Least Squares Difference (LSD) post-hoc comparisons were performed to determine the specific turbulence intensities that evoked behavioral changes within each species (Zar, 1999).

3. Results

3.1. Transport speeds of copepods

The observed movements of the copepods in the still and turbulent flow conditions define the transport velocities. Data were normally distributed for each of the three species tested at each of the five strain rate levels and untransformed data were analyzed. The two-way ANOVA showed significant effects due to strain rate ($F_{4,178}=39.9$, $p<0.001$), species ($F_{2,178}=3.8$, $p<0.05$), and the interaction of strain rate * species ($F_{8,178}=6.77$, $p<0.001$). The one-way ANOVA showed significant effects of strain rate on all 3 species: *A. hudsonica* ($F_{4,52}=14.4$, $p<0.001$), *T. longicornis* ($F_{4,72}=4.37$, $p<0.005$), and *C. finmarchicus* ($F_{4,54}=48.5$, $p<0.001$). For each species, the transport velocity peaked at an intermediate turbulence level between $\sigma_{rms}=0.24\ s^{-1}$ and $0.79\ s^{-1}$ (Fig. 3). The maximum observed transport velocity occurred at T3 (*A. hudsonica* and *T. longicornis*) and at T2 (*C. finmarchicus*).

3.2. Motility number

Gallager et al. (2004) defined the motility number, Mn, as the observed copepod transport speed divided by the r.m.s. of the turbulent fluid velocity, and we also calculated this quantity to compare copepod responses to turbulence in the laboratory to those observed in the field (Fig. 4, shown versus dissipation rate). For this analysis, the lowest turbulence level of still water was excluded since the r.m.s. velocity was zero. The two-way ANOVA indicated an insignificant effect of species ($F_{2,148}=0.71$, $p>0.05$) with significant effects of strain rate ($F_{3,148}=67.9$, $p<0.001$) and species * strain rate interaction ($F_{6,148}=5.3$, $p<0.001$). Hence, there is an effect of strain rate, and the interaction indicates that the effect of strain rate is contingent on species. One-way ANOVA showed significant decreases in Mn with increases in turbulence intensity for each species (*A. hudsonica*: $F_{3,40}=46.7$, $p<0.001$, *T. longicornis*: $F_{3,59}=37.2$, $p<0.001$, *C. finmarchicus*: $F_{3,49}=14.2$, $p<0.001$). Mn declined monotonically with strain rate for *A. hudsonica* and *T. longicornis*. In contrast, Mn in *C. finmarchicus* showed a threshold-like relationship to strain rate; Mn increased until T2, then declined to a constant level at T3 and T4.

In the studies of Gallager et al. (2004), they observed that copepods in the ocean could aggregate for Mn greater than three, whereas they did not aggregate when Mn was smaller. Thus, if Mn is greater than three, then plankton behavior dominates over the physical forcing, i.e. the copepod can swim through the flow field. In the current data, Mn for T1 and T2 was greater than three, and Mn was less than three for T3 and T4 (Fig. 4), suggesting a possible parallel between field and laboratory responses. Continued use of this index will contribute to building this database for future comparisons.

3.3. Variation in observed copepod transport speeds

As turbulence increases, the r.m.s. of the fluid velocity increases by roughly a factor of nine (Table 1). It is important to distinguish that the fluid velocity fluctuations were measured from an Eulerian perspective (i.e. fixed perspective) and transport speed was calculated from the Lagrangian perspective where the time sequence of velocity data corresponded to an individual copepod trajectory. This is in contrast with the Eulerian perspective that would correspond to a time record of many copepods moving past a fixed point in the field.

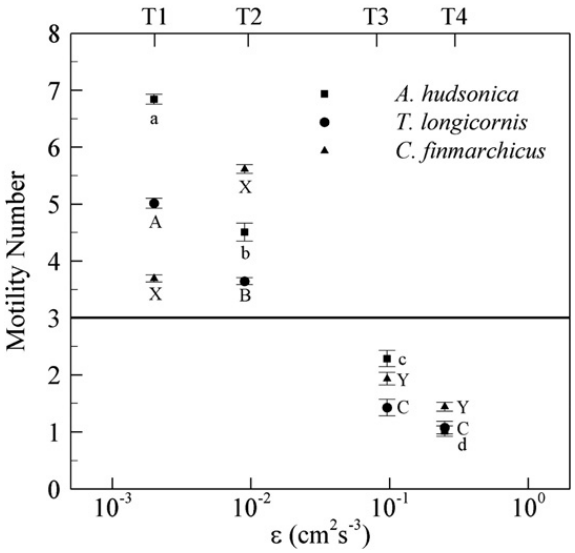

Fig. 4. Motility number as a function of turbulence intensity. Data points above the horizontal line at Mn=3 indicate that copepod swimming dominates over physical transport (Gallager et al., 2004). Letters indicate treatments that are not significantly different using a Tukey–Kramer test, $p<0.05$.

The standard deviation provides a measure of the variability of the transport speed along the trajectory and was calculated for each trajectory. Fig. 5 reports the average of all trajectories for each T-level. The data were arcsine transformed to conform to the assumptions of normality. The two-way ANOVA showed significant effects of species ($F_{2,178}=63.9$, $p<0.001$) and strain rate levels ($F_{4,178}=20.9$, $p<0.001$) as well as a significant species*strain rate interaction ($F_{8,178}=9.6$, $p<0.001$). The one-way ANOVA showed no significant differences for any of the pairwise comparisons for *A. hudsonica* and *T. longicornis* indicating strain rate was not a significant factor in the responses of either *A. hudsonica* ($F_{4,52}=2.2$, $p=0.081$) or *T. longicornis* ($F_{4,72}=0.49$, $p>0.05$). It may be assumed that samples within these data sets were statistically coincident. The one-way ANOVA showed significant effect of strain rate on standard deviation for *C. finmarchicus* ($F_{4,54}=329.3$, $p<0.001$). Thus, for the smaller copepods, *A. hudsonica* and *T. longicornis*, the standard deviation of transport speed is nearly constant with increasing turbulence. In contrast, for the larger copepod *C. finmarchicus*, the standard deviation increases by roughly a factor of five at strain rates greater than 0.24 s^{-1} (Fig. 5).

3.4. Net-to-gross-displacement ratio

Net-to-gross-displacement ratio was calculated for 1-second trajectories to compare the tortuosity of the trajectories between species and among turbulence levels (Fig. 6). The data used to analyze the effects of five levels of turbulence on NGDR for three species were arcsine transformed to conform to the assumptions of normality. The two-way ANOVA showed significant effects of species ($F_{2,57}=43.3$, $p<0.001$) and species*strain rate interaction ($F_{8,57}=4.36$, $p<0.001$) and no effect of strain rate level ($F_{4,57}=1.01$, $p=0.415$). The one-way ANOVA showed a strong trend for the effect of strain rate on NGDR for both *A. hudsonica* ($F_{4,19}=2.24$, $p=0.103$) and *T. longicornis* ($F_{4,20}=2.30$, $p=0.095$) with trajectories becoming more linear with increasing strain rate. The one-way ANOVA showed significant effects of strain rate on the NGDR for the largest copepod, *C. finmarchicus* ($F_{4,18}=4.76$, $p<0.05$) with trajectories becoming more tortuous with increasing strain rate above 0.24 s^{-1}. The opposing trends for the three species accounts for the lack of a strain rate effect in the two-way ANOVA.

3.5. Copepod escape behavior

Escape responses were measured by observing randomly-selected individual copepods and counting the

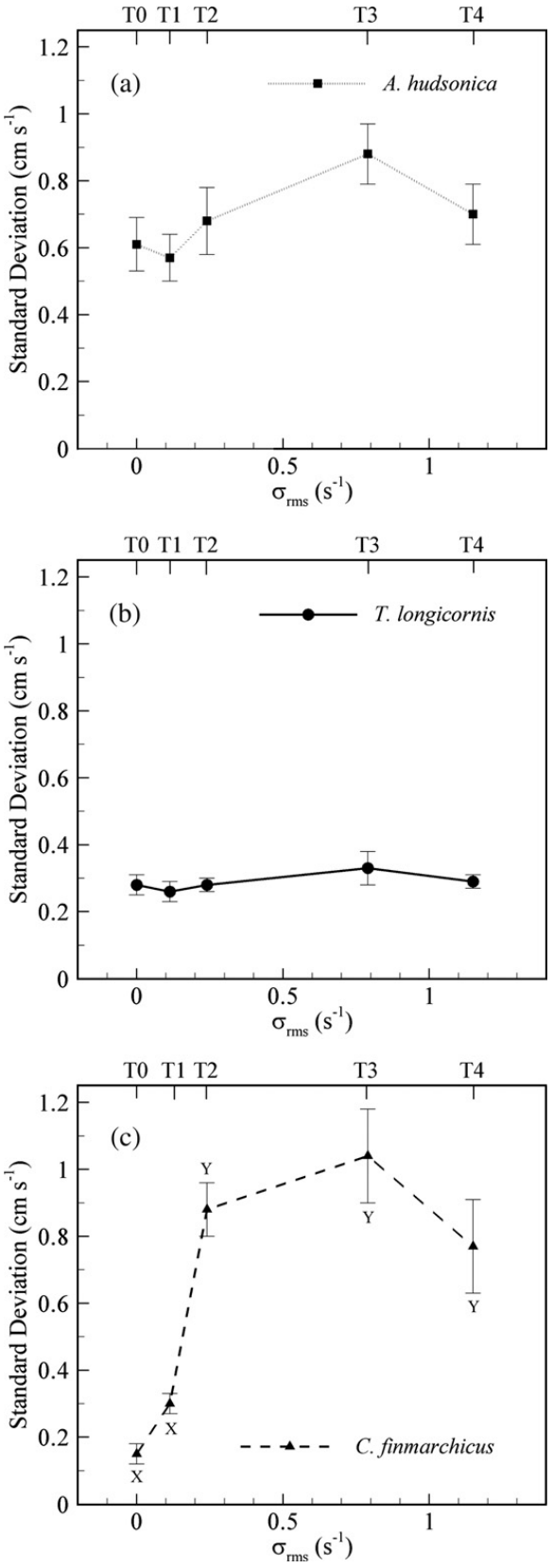

Fig. 5. Standard deviation of transport speed (a) *A. hudsonica*, (b) *T. longicornis*, and (c) *C. finmarchicus*. Letters indicate treatments that are not significantly different using a Tukey–Kramer test, $p<0.05$. Statistical analyses were performed on arc-sine transformed data.

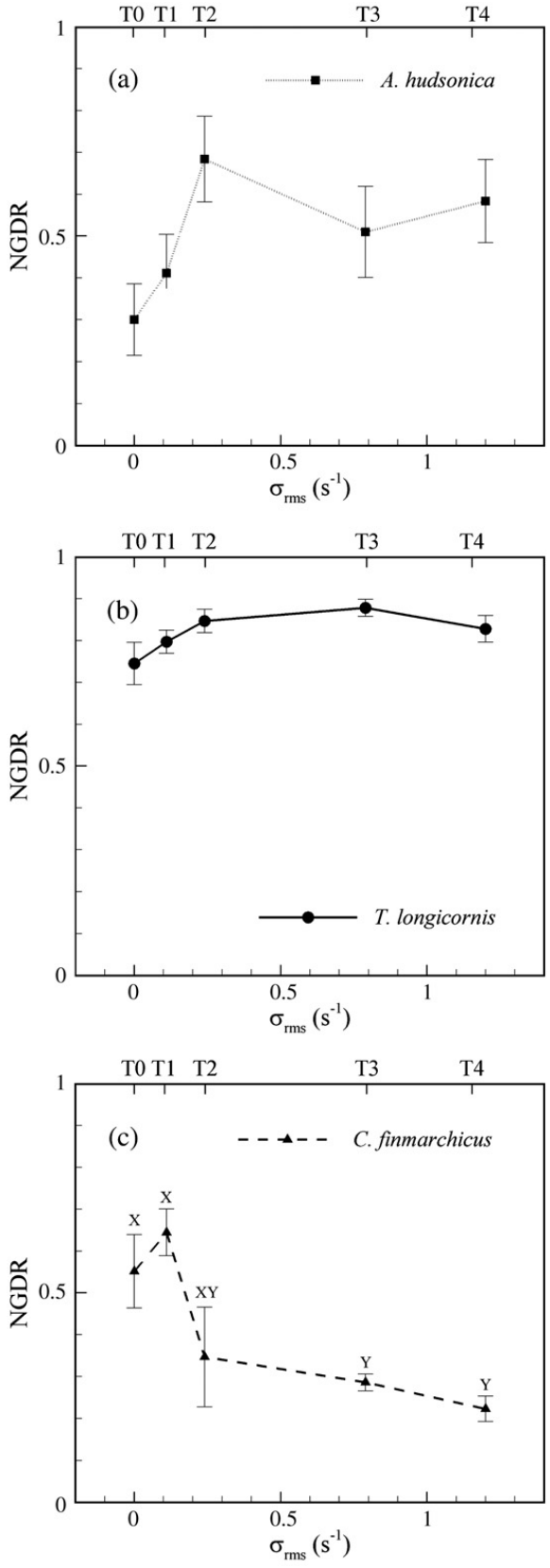

Fig. 6. Net-to-gross-displacement ratio (NGDR) for (a) *A. tonsa*, (b) *T. longicornis*, and (c) *C. finmarchicus*. Letters indicate treatments that are not significantly different using a Tukey–Kramer test, $p<0.05$. Statistical analyses were performed on arc-sine transformed data.

number of escapes that they exhibited during 5-second intervals. An escape is characterized by an abrupt and sudden movement by the copepod. A total of 200 5-second intervals were evaluated for the escape analysis for each turbulence level. To conform to the assumptions of normality, the data used to analyze the effects of 5 levels of turbulence on the escape response of three copepod species were transformed, using the square root transformation. The two-way ANOVA showed significant effects of species ($F_{2,1485}=180.4$, $p<0.001$) as well as a significant species * strain rate interaction ($F_{8,1485}=4.34$, $p<0.001$), but no effect of strain rate ($F_{4,1485}=1.07$, $p=0.37$). The one-way ANOVA showed significant, but opposing, effects of strain rate on two species, which accounts for the lack of a significant effect of strain rate when analyzed with the two-way ANOVA. For *A. hudsonica*, there were more escapes at T0 and T1 compared to the higher T-levels, which were statistically coincident ($F_{4,495}=5.2$, $p<0.001$). For *T. longicornis*, there were no significant differences among the pairwise comparisons for escape data ($F_{4,495}=0.89$, $p=0.471$). For *C. finmarchicus,* there were more escapes at the higher T-levels compared to T1 ($F_{4,495}=3.73$, $p<0.05$).

A. hudsonica exhibited escape behavior more often for all turbulence levels than *T. longicornis* and *C. finmarchicus*. *A. hudsonica* exhibited the most escapes for T1 (3.3 escapes/5 s/copepod) and the number of escapes decreased at higher turbulent intensities above the fluctuating strain rate r.m.s. of 0.24 s^{-1}. The escape behavior of *T. longicornis* showed no relationship with strain rate. *T. longicornis* escaped at a frequency around

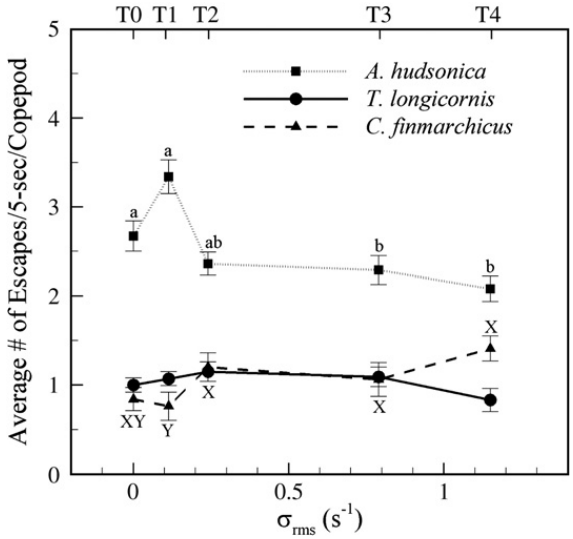

Fig. 7. Number of escape events per 5-second interval per copepod. Letters indicate treatments that are not significantly different using a Tukey–Kramer test, $p<0.05$. Statistical analyses were performed on square root transformed data.

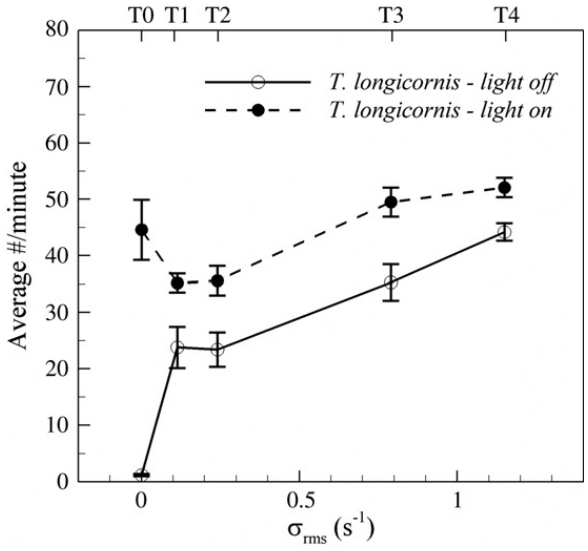

Fig. 8. Average number of copepods in field of view per minute for light-on and light-off conditions for *T. longicornis*.

1 escape/5 s/copepod for all turbulence levels (Fig. 7). As strain rate increased above 0.24 s^{-1}, the number of escapes of *C. finmarchicus* increased.

3.6. Copepod aggregation to the light source

We assessed the ability of *T. longicornis* to aggregate around a light beam while being exposed to turbulence by counting the number of copepods in the vicinity of the beam (within a window of 9.5 × 7.5 cm) per minute for each T-level. *T. longicornis* exhibited a positive phototactic response to the light source, but as turbulence intensity increased, its ability to aggregate to the light source diminished. For the T0 conditions without the laser beam projecting through the box, the number of copepods was very small (Fig. 8). For T0, the number for light-off and light-on conditions was significantly different based on a *t*-test ($p < 0.001$). The addition of turbulence increased the number of *T. longicornis* in the observation window per minute (Fig. 8) for the light-off conditions due to increased stirring. The average number of copepods in view per minute was higher with the light-on for each T-level.

4. Discussion

Many studies (e.g. MacKenzie et al., 1994; Dower et al., 1997; Saiz et al., 2003) suggest that parameters, such as plankton ingestion rate, follow a dome-shaped trend with increasing turbulence. Mechanistically, the increase has been attributed to increased contact rate (Rothschild and Osborn, 1988) while the decrease at high turbulence has been ascribed to several factors: 1. erosion of the feeding current and sensory field, 2. energy-costly reactions to turbulence (e.g. escapes) limiting the energy or time needed for other survival responses (successful foraging or mating), 3. physically-induced transport surpassing behavioral reaction times, thus decreasing the probability of successful pursuit once an encounter has occurred, as found by MacKenzie et al. (1994) for larval fish. In our study, considering factor 1 at higher turbulence intensities, the 9-fold increase in u_{rms} results in little change and even a slight decline in the copepod transport speeds. The motility number Mn shows that at higher turbulence intensities, the physical flow dominates over biologically controlled propulsion. With no copepod-generated movement, it is unlikely that a cruising copepod, as is *T. longicornis*, has a self-generated flow field or has the ability to stabilize a useful sensory field. Instantaneously, copepods that have not been fatigued may be transported momentarily by the physical flow yet still be able to rebuild its sensory field in the less active flow regions. For factor 2, none of the species in this study exhibited a large change in escape frequency with increased turbulence intensities. All events were examined after exposure to turbulence for more than 10 min, allowing time for habituation and fatigue. Under these conditions, *A. hudsonica* was able to maintain its species-specific higher hop frequencies. *T. longicornis* and *C. finmarchicus*, on the other hand, showed little change in behavior suggesting that costly escapes are not a behavior evoked within this range of turbulence intensity. The species-specific behavior is intriguing and closer analyses of behavioral budgets may provide insight on changes in the behavioral repertoire with increases in physical flow disturbances. As for reaction times (factor 3), physiologically, copepods are able to react in a few milliseconds (Fields et al., 2002). However, good estimates of the amount of time that interacting copepods remain correlated are not available to assess the role of reaction time.

Despite lacking an obvious mitigating factor, observed transport speed was not constant over the range of turbulence tested. Chamorro (2001) showed a nonlinear dome-shaped variation of larval fish swimming speed to turbulence with and without food and suggested that the larvae lose their ability to swim and control their position in high turbulence. Several trends reported in our study support the application of the dome-shaped response as a model of the kinematic behavioral response of copepods to turbulence. The observed transport speed of all three species was highest at an intermediate turbulence intensity. Further, the motility number suggests that for low

turbulence intensities (T1 and T2), copepod behavior may dominate over the physical flow, whereas for higher turbulence (T3 and T4) the physical transport of the flow dominated. In our studies, the transition occurred at a dissipation rate of 9×10^{-3} cm^2 s^{-3} and a strain rate r.m.s. value of 0.24 s^{-1}. Since fatigue can be a factor, trends may be different for copepods with shorter exposure times to turbulence. These results are consistent with the assumption of Yamazaki and Squires (1996) that plankton with swimming speeds higher than the turbulent velocity can be expected to exhibit motion independent of the surrounding flow, while the motion of plankton with swimming speed lower than the turbulence should be driven by the local flow. Further, Levandowsky et al. (1988) predicted that when a microzooplankter′s swimming speed is less than the turbulent velocity, it is advantageous to be carried by the flow to minimize the overlap of search volumes. Our studies find that each species′ behavior (transport speed, NGDR, SD, #escapes) showed different trends (increase, decrease, dome-shaped) that may reflect species-specific responses to turbulence.

In turbulent flows, Saiz and Alcaraz (1992) and Hwang et al. (1994) observed increased jump frequency with increased turbulence for *Acartia clausi* and *C. hamatus*, respectively. In contrast, Saiz (1994) observed that *A. tonsa* did not increase its jump frequency for increased turbulence. These experiments were conducted in the presence of food, thus the jump response may have been influenced by the proximity of food particles. The absence of food particles in the current experiments isolates the response to mechanoreception of the fluctuating flow field. Furthermore, in our studies, copepods were exposed to the turbulent velocities for over 10 min before their instantaneous responses were analyzed, thus integrating the effect of fatigue and habituation, as might occur in a storm at sea. Since *Acartia* sp. is a hop and sink traveler (Mauchline, 1998), more escapes were expected for *A. hudsonica* than the other tested species. Indeed, the data show that *A. hudsonica* escaped more frequently for all turbulence levels compared to *T. longicornis* and *C. finmarchicus*. *A. hudsonica* was most reactive at an intermediate turbulence intensity. *T. longicornis* did not have a substantial variation of escape reactions across the turbulence intensity levels. *C. finmarchicus* had the highest escape frequency at the highest intensity. Species specificity in copepod responses to turbulence is suggested by these data.

Fields and Yen (1997) state that most copepods exhibit an escape reaction to an apparent predation risk. The turbulent flow fluctuations for those conditions may mimic the disturbance created by their predators or prey, thereby inducing an escape reaction. Escape response in laminar flow is best correlated with strain rate rather than other flow parameters, such as flow velocity magnitude (Fields and Yen, 1997; Kiørboe et al., 1999). The local maximum for *A. hudsonica* suggests that the strain rate perturbations for T1 most closely mimic that created by their predators or prey.

To test the effect of turbulence on a specific behavior, we placed an attractive cue in the center of our field of view, a green beam of light, to evoke phototaxis. *T. longicornis* responded strongly, swarming around the light beam and increasing its numbers in the viewing region. While the statistically significant difference between the average number of copepods in the field of view per minute for the conditions of light-on and light-off with increasing turbulence decreased, this aggregative behavior persisted even at the highest turbulence level. Here is an example where biological forcing affecting the copepod′s distribution and dominated over physical forces.

In the ocean, the vertical distribution of plankton is guided by many factors: biological, chemical, and physical. The ability of organisms to partition vertically suggests that pelagic ecosystems are highly structured (e.g. Manning and Bucklin, 2005). The influence of turbulence on vertical partitioning has been enigmatic. Since turbulence intensity diminishes significantly with depth, copepod species at different depths experience different flow environments. Analysis of copepod trajectories demonstrated that the size and swimming style of the copepod influence their behavior in turbulent waters. We discuss the species-specific effects, considering the smallest to largest copepods. Trajectories of the smallest species, *A. hudsonica*, became straighter with increased turbulence (strong trend). The increased straightness of the trajectories for *A. hudsonica* suggests that the smaller copepod was passively transported by the flow as the turbulence intensity increased (see simulated trajectories in Yamazaki et al., 1991). In contrast, the middle-sized copepod, *T. longicornis* was able to maintain its smooth swimming, showing little change in the standard deviation of transport speed. This copepod also moved along paths of similar complexity (NGDR values were constant with respect to turbulence level). This species showed no change in hop frequency. Furthermore, *T. longicornis* was able to maintain its phototactic behavior and exhibit its biologically-motivated aggregative response even at the highest turbulence intensity. Our expectation is that *T. longicornis* would be able to continue its searching behavior and benefit from turbulence within this range. The largest species,

C. finmarchicus, was stronger and better equipped (by size) to overcome the flow field. Trajectories for *C. finmarchicus* became more tortuous with increasing turbulence, which is consistent with trajectories that include swimming behavior in addition to flow transport (Yamazaki et al., 1991). Variation, quantified as the standard deviation of the transport speed, also increased at the higher turbulence intensities. However, at the highest turbulence intensity, the variations in speeds showed a decline whereas path complexity continued to increase. The results for *C. finmarchicus* suggest an ability to adjust their heading frequently in response to the local flow field. The larger body mass with stronger propulsive capability may enable this copepod to change its behavior with a consequence of staying in the same region. Are these large copepods conditioned to react to turbulence by increasing their turning frequency to stay in the same region and experience the benefits of increased contact rate with food? Field data show that the abundance of *Calanus* often peaks in periods of high turbulence (Manning and Bucklin, 2005). It is intriguing to consider whether this larger copepod invests energy to remain in the same region by swimming against the fluctuations and thus avoids being transported out of the more turbulent regime. In summary, turbulence appears to affect each copepod in a species-specific manner, and the impact on the *in situ* distribution and abundance may require a careful consideration of the combined responses to turbulent flow. The trends from these quantitative analyses now can be compared to responses of copepods exposed to varying turbulence durations.

The purpose of this paper is to report use of a new apparatus that permits simultaneous detailed observations of plankton behavior and turbulent velocities. To test copepod response to turbulent flow motions, additional experiments are recommended. Comparison of the transport of inert particles compared to freely swimming copepods will definitely distinguish the influence of turbulence on swimming kinematics. Copepods found at different turbulence horizons can be studied in the lab for their behavioral responses to these specific turbulence levels. Differential species responses assessed in the laboratory should be reflected in their field distributions, hence linking the laboratory observations to the field distributions. Additional questions remain regarding variation in copepod response to turbulence possibly due to water temperature, diel migration to the surface at dusk and dawn, activity level during different seasons, and stomach fullness. Since the apparatus has optical access, future measurements of high speed high magnification views of copepods within the field of isotropy can reveal the deployment or lack of use of swimming legs at different turbulence intensities. Most importantly, it would be highly desirable to measure the instantaneous flow field in the region surrounding the copepod in order to directly correlate velocity fluctuations to animal behavior to properly assess the contribution due to transport and biologically-generated propulsion.

Acknowledgements

Special thanks to Marc Weissburg and C. Brock Woodson for guidance with the statistical analysis. Thanks to Michael Doall and Jeff Levinton (State University of New York — Stony Brook) and Ann Bucklin and Chris Manning (University of New Hampshire) for animal collection and shipment. Thanks also to J. Rudi Strickler and Jason Brown for design and construction of the shadowgraph system. This manuscript has been improved based on many of the referees′ comments. Our research was partially funded by Office of Naval Research grant #N000140310366.

References

Apstein, C., 1910. Hat ein Organismus in der tiefe gelebt, in der er gefischt ist? Int. Rev. Gesamten Hydrobiol. Hydrograph. 3, 17–33.

Boxshall, G.A., Yen, J., Strickler, J.R., 1997. Functional significance of the sexual dimorphism in the cephalic appendages of *Euchaeta rimana* Bradford. Bull. Mar. Sci. 61, 387–398.

Buskey, E.J., Swift, E., 1985. Behavioral responses of oceanic zooplankton to simulated bioluminescence. Biol. Bull. 168, 263–275.

Buskey, E., Mills, L., Swift, E., 1983. The effects of dinoflagellate bioluminescence on the swimming behavior of a marine copepod. Limnol. Oceanogr. 28, 575–579.

Chamorro, V.C., 2001. The effects of small scale turbulence in the feeding ecology and swimming speed of fathead minnow larvae (*Pimephales promelas*), inland silverside larvae (*Menidia beryllina*) and the lobate ctenophore (*Mnemiopsis leidyi*). M.S. Thesis. University of Maryland. College Park, Maryland.

Dicke, M., Burrough, P.A., 1988. Using fractal dimensions for characterizing tortuosity of animal trails. Physiol. Entomol. 13, 393–398.

Dower, J.F., Miller, T.J., Leggett, W.C., 1997. The role of microscale turbulence in the feeding ecology of larval fish. Adv. Mar. Biol. 31, 169–220.

Fields, D.M., Yen, J., 1997. The escape behavior of marine copepods in response to a quantifiable fluid mechanical disturbance. J. Plankton Res. 19, 1289–1304.

Fields, D.M., Shaeffer, D.S., Weissburg, M.J., 2002. Mechanical and neural responses from the mechanosensory hairs on the antennule of *Gaussia princeps*. Mar. Ecol., Prog. Ser. 227, 173–186.

Franks, P.J.S., 2001. Turbulence avoidance: an alternate explanation of turbulence-enhanced ingestion rates in the field. Limnol. Oceanogr. 46, 959–963.

Galbraith, P.S., Browman, H.I., Racca, R.G., Skiftesvik, A.B., Saint-Pierre, J.-F., 2004. Effect of turbulence on the energetics of

foraging in Atlantic cod *Gadus morhua* larvae. Mar. Ecol., Prog. Ser. 281, 241–257.

Gallager, S.M., Yamazaki, H., Davis, C.S., 2004. Contribution of fine-scale vertical structure and swimming behavior to formation of plankton layers on Georges Bank. Mar. Ecol., Prog. Ser. 267, 27–43.

Granata, T.C., Dickey, T.D., 1991. The fluid mechanics of copepod feeding in a turbulent flow: a theoretical approach. Prog. Oceangr. 26, 243–261.

Gross, F., Raymont, J.E.G., 1942. The specific gravity of *Calanus finmarchicus*. Proc. R. Soc. Edinb. 61B, 288–296.

Haury, L.R., Yamazaki, H., Itsweire, E.C., 1990. Effects of turbulent shear flow on zooplankton distribution. Deep-Sea Res., A 37, 447–461.

Heath, M.R., Henderson, E.W., Baird, D.L., 1988. Vertical distribution of herring larvae in relation to physical mixing and illumination. Mar. Ecol., Prog. Ser. 47, 211–228.

Hirche, H.-J., 1987. Temperature and plankton. II. Effect on respiration and swimming activity in copepods from the Greenland Sea. Mar. Biol. 94, 347–356.

Hwang, J.-S., Costello, J.H., Strickler, J.R., 1994. Copepod grazing in turbulent flow: elevated foraging behavior and habituation of escape responses. J. Plankton Res. 16, 421–431.

Incze, L.S., Hebert, D., Wolff, N., Oakey, N., Dye, D., 2001. Changes in copepod distributions associated with increased turbulence from wind stress. Mar. Ecol., Prog. Ser. 213, 229–240.

Jiménez, J., 1997. Oceanic turbulence at millimeter scales. Sci. Mar. 61 (suppl. 1), 47–56.

Jonsson, P.R., Tiselius, P., 1990. Feeding behavior, prey detection and capture efficiency of the copepod *Acartia tonsa* feeding on planktonic ciliates. Mar. Ecol., Prog. Ser. 60, 35–44.

Kiørboe, T., Saiz, E., 1995. Planktivorous feeding in calm and turbulent environments, with emphasis on copepods. Mar. Ecol., Prog. Ser. 122, 135–145.

Kiørboe, T., Saiz, E., Visser, A., 1999. Hydrodynamic signal perception in the copepod *Acartia tonsa*. Mar. Ecol., Prog. Ser. 179, 97–111.

Lagadeuc, Y., Boule, M., Dodson, J.J., 1997. Effect of vertical mixing on the vertical distribution of copepods in coastal waters. J. Plankton Res. 19, 1183–1204.

Landry, M.R., Fagerness, V.L., 1988. Behavioral and morphological influences on predatory interactions among marine copepods. Bull. Mar. Sci. 43, 509–529.

Levandowsky, M., Klafter, J., White, B.S., 1988. Feeding and swimming behavior in grazing microzooplankton. J. Protozool. 35, 243–246.

Lewis, D.M., 2005. A simple model of plankton population dynamics coupled with a LES of the surface mixed layer. J. Theor. Biol. 234, 565–591.

Mackas, D.L., Sefton, H., Miller, C.B., Raich, A., 1993. Vertical habitat partitioning by large calanoid copepods in the oceanic subarctic Pacific during spring. Prog. Oceanogr. 32, 259–294.

MacKenzie, B.R., 2000. Turbulence, larval fish ecology and fisheries recruitment: a review of field studies. Oceanol. Acta 23, 357–375.

MacKenzie, B.R., Miller, T.J., Cyr, S., Leggett, W.C., 1994. Evidence for a dome-shaped relationship between turbulence and larval fish ingestion rates. Limnol. Oceanogr. 39, 1790–1799.

Manning, C.A., Bucklin, A., 2005. Multivariate analysis of the copepod community of near-shore waters in the western Gulf of Maine. Mar. Ecol., Prog. Ser. 292, 233–249.

Marrasé, C., Saiz, E., Redondo, J.M. (Eds.), 1997. Lectures on Plankton and Turbulence. Sci. Mar., vol. 61 (Suppl. 1), pp. 1–238.

Mauchline, J., 1998. The Biology of Calanoid Copepods. Elsevier Academic Press, San Diego, California.

Peters, F., Marrasé, C., 2000. Effects of turbulence on plankton: an overview of experimental evidence and some theoretical considerations. Mar. Ecol., Prog. Ser. 205, 291–306.

Rasberry, K.D., 2005. The behavioral effect of laboratory turbulence on copepods. M.S. Thesis, Georgia Institute of Technology. Atlanta, Georgia.

Rothschild, B.J., Osborn, T.R., 1988. Small-scale turbulence and plankton contact rates. J. Plankton Res. 10, 465–474.

Saiz, E., 1994. Observations of the free-swimming behavior of Acartia tonsa: effects of food concentration and turbulent water motion. Limnol. Oceanogr. 39, 1566–1578.

Saiz, E., Alcaraz, M., 1992. Free-swimming behavior of *Acartia clausi* (Copepoda: Calanoida) under turbulent water movement. Mar. Ecol., Prog. Ser. 80, 229–236.

Saiz, E., Kiørboe, T., 1995. Predatory and suspension feeding of the copepod *Acartia tonsa* in turbulent environments. Mar. Ecol., Prog. Ser. 122, 147–158.

Saiz, E., Calbet, A., Broglio, E., 2003. Effects of small-scale turbulence on copepods: the case of *Oithona davisae*. Limnol. Oceanogr. 48, 1304–1311.

Titelman, J., 2001. Swimming and escape behavior of copepod nauplii: implications for predator–prey interactions among copepods. Mar. Ecol., Prog. Ser. 213, 203–213.

Visser, A.W., 2001. Hydromechanical signals in the plankton. Mar. Ecol., Prog. Ser. 222, 1–24.

Visser, A.W., Stips, A., 2002. Turbulence and zooplankton production: insights from PROVESS. J. Sea Res. 47, 317–329.

Visser, A.W., Saito, H., Saiz, E., Kiørboe, T., 2001. Observations of copepod feeding and vertical distribution under natural turbulent conditions in the North Sea. Mar. Biol. 138, 1011–1019.

Webster, D.R., Brathwaite, A., Yen, J., 2004. A novel apparatus for simulating isotropic oceanic turbulence at low Reynolds number. Limnol. Oceanogr.: Methods 2, 1–12.

Weissman, P., Lonsdale, D.J., Yen, J., 1993. The effect of peritrich ciliates on the production of *Acartia hudsonica* in Long Island Sound. Limnol. Oceanogr. 38, 613–622.

Woodson, C.B., Webster, D.R., Weissburg, M.J., Yen, J., 2005. Response of copepods to physical gradients associated with structure in the ocean. Limnol. Oceanogr. 50, 1552–1564.

Yamazaki, H., 1996. Turbulence problems for planktonic organisms. Mar. Ecol., Prog. Ser. 139, 304–305.

Yamazaki, H., Squires, K.D., 1996. Comparison of oceanic turbulence and copepod swimming. Mar. Ecol., Prog. Ser. 144, 299–301.

Yamazaki, H., Osborn, T.R., Squires, K.D., 1991. Direct numerical simulation of planktonic contact in turbulent flow. J. Plankton Res. 13, 629–643.

Yen, J., Fields, D.M., 1992. Escape responses of *Acartia hudsonica* (Copepoda) nauplii from the flow field of *Temora longicornis* (Copepoda). Arch. Hydrobiol., Beih. 36, 123–134.

Yen, J., Lenz, P.H., Gassie, D.V., Hartline, D.K., 1992. Mechanoreception in marine copepods: electrophysiological studies on the first antennae. J. Plankton Res. 14, 495–512.

Zar, J.H., 1999. Biostatistical Analysis, 4th edition. Prentice Hall, Upper Saddle River, New Jersey.